Journal of Radiation Research and Applied Sciences 8 (2015) 393–398

HOSTED BY

Available online at www.sciencedirect.com

ScienceDirect

Journal of Radiation Research and Applied Sciences

journal homepage: http://www.elsevier.com/locate/jrras

Measurement of natural radioactivity in granites and its quartz-bearing gold at El-Fawakhir area (Central Eastern Desert), Egypt

M.A.M. Uosif [a,*], Shams A.M. Issa [a,b], L.M. Abd El-Salam [c]

[a] Physics Department, Faculty of Sciences, Al-Azhar University (Assiut branch), Egypt
[b] Physics Department, Faculty of Sciences, Tabuk, Saudi Arabia
[c] Geology Department, Faculty of Sciences, Al-Azhar University (Assiut branch), Egypt

ARTICLE INFO

Article history:
Received 31 August 2014
Received in revised form
26 January 2015
Accepted 18 February 2015
Available online 4 March 2015

Keywords:
Natural radionuclides
Granite rocks
Radiological Hazards
Excess lifetime cancer risks

ABSTRACT

The distribution of natural radionuclides (^{226}Ra, ^{232}Th and ^{40}K) in Granites and its quartz-bearing gold at El-Fawakhir area (Central Eastern Desert, Egypt) were measured by using γ-ray spectroscopy [NaI (Tl) 3″ × 3″]. X-Ray Fluorescence technique was used for chemical analyses of the studied samples. The specific activity of ^{226}Ra, ^{232}Th and ^{40}K values are in range (3 ± 0.5 to 43 ± 2 Bqkg^{-1}), (5 ± 0.7 to 41 ± 2 Bqkg^{-1}) and (128 ± 6 to 682 ± 35 Bqkg^{-1}) respectively. The absorbed dose rates ranged from 13.8 to 58.4 nGy h^{-1}, where the total effective dose rates were determined to be between 16.7 and 70.9 μSvy^{-1}. The maximum external hazard index (H_{ex}) is 0.3 nGyh^{-1}. The calculated values of the excess lifetime cancer risks (ELCR) and annual effective dose rate values are in between (8.48×10^{-5} and 2.63×10^{-4}) and (24.2 and 72.9 μSvy^{-1}) respectively. Geochemically, the studied granites consist of major oxides, they are characterized by SiO_2, K_2O, Na_2O, Al_2O_3, and depleted in CaO, MgO, TiO_2, and P_2O_5. The average absorbed dose rate (D_o) in air is 37.8 nGyh^{-1} for the whole studied samples, this value is about 3.78% of the 1.0 mSvy^{-1} recommended by (ICRP-60,1991) to the public, so there is no radiological risk for the workers in that area.

1. Introduction

When the earth was formed four billion years ago, it contained many radioactive isotopes. Since then, all the shorter lived isotopes have decayed. Only those isotopes with very long half-lives (100 million years or more) remain, along with the isotopes formed from the decay of the long lived isotopes. Background radiation is the ubiquitous ionizing radiation that people on the planet Earth are exposed to, including natural and artificial sources. Both natural and artificial background radiation varies depending on location and altitude. Every day, we ingest/inhale nuclides in the air we breathe, in the food we eat and in the water we drink. Radioactivity is common in the rocks and soil that make up our planet, in the water and oceans, and even in our building materials and homes. It is just everywhere (Uosif & Abdel-Salam, 2011).

* *Corresponding author.*
E-mail address: dr_mohamed_amin@lycos.com (M.A.M. Uosif).
Peer review under responsibility of The Egyptian Society of Radiation Sciences and Applications.
http://dx.doi.org/10.1016/j.jrras.2015.02.005

Granite's durability and decorative appearance make it a popular building material in homes and buildings. Any type of rock could contain naturally occurring radioactive elements like radium, uranium and thorium. Some pieces of granite contain more of these elements than others, depending on the composition of the molten rock from which they formed. Geologists provide an explanation of this behavior in the course of partial melting and fractional crystallization of magma, which enables U and Th to be concentrated in the liquid phase and become incorporated into the more silica-rich products. For that reason, igneous rocks of granitic composition are strongly enriched in U and Th (on an average 5 ppm of U and 15 ppm of Th), compared to the Earth's crust (average 1.8 ppm for U and 7.2 ppm for Th) (Mason & Moore, 1982), the upper continental crust (average 2.7 ppm for U and 10.5 ppm for Th) (Rudnick & Gao, 2003) and rocks of basaltic or ultramafic composition (0.1 ppm of U and 0.2 ppm of Th) (Faure, 1986) and (Me'nager et al. 1993).

The Fawakhir granite is a stock intruded into the older Precambrian rocks. As no agriculture has ever succeeded in this hyperarid desert, the only resources are mineral, namely, gold, granite, and water. The granite was quarried to no great extent in the Roman period, but it also acts as an aquifer, carrying water in tiny cracks until it is stopped by the dense ultramafic rocks to the west. Most importantly, however, the quartz veins injected into the granite are auriferous, particularly towards the edge of the stock. The present work deals with the radioactivity and radiological hazard of El Fawakhir mining area.

2. Geological setting

El-Fawakhir granite platoon hosts and El-Fawakhir gold mines, which are two of several gold mines in the Eastern Desert of Egypt that have been extensively worked since Pharaonic and Roman times (Amer, Kusky, & Ghulam, 2008). The rock varieties encountered from the oldest to the youngest are meta-sediments, gabbroic sheet, younger granites and Quaternary Wadi deposits. The Carbonic sheet is grayish brown in color on the weathered surface and intruded by younger granites to the central part of the studied area. The volcanic rocks (40%) are located around El-Fawakhir granites and running east to west, Fig. 1.

The Gold pockets in the El-Fawakhir quarry in the Eastern side of the studied area. There are two points of view regarding the genesis of the known gold mineralization in the Eastern Desert of Egypt. Some authors discussed the gold mineralization genesis based on the geosynclinals theory (El-Shazly, 1956; Sabet, Tosgeov, Bordonosov, Baburin, & Zalta, 1976). Recently, some authors linked the gold mineralization to the plate tectonic theory (Hassan, 2006; Hassan, Azzaz, Soliman, El-Badway, 1991) under ophiolite, island arc and cordilleran-extensional, group. Each possesses characteristic ore mineral assemblage and geochemical association. Several Gold deposit and plugs are recorded in the studied area. The Gold pockets in the El-Fawakhir quarry in the Eastern side of the studied area. There are two points of view regarding the genesis of the known gold mineralization in the Eastern Desert of Egypt. Some authors discussed the gold mineralization genesis based on the geosynclinals theory (El-Shazly, 1956). Some authors linked the gold mineralization to the plate tectonic theory (Hassan, 2006; Sabet et al., 1976) under ophiolite, island arc and cordilleran-extensional, group. Each possesses characteristic ore mineral assemblage and geochemical association.

Veins: The study area is traversed by gold-bearing quartz veinlets. The main occurrences are those at El Fawakhir main quartz veins are exploited for gold. These quartz veinlets represent the second stage of the heat engine process affecting the area and lead to the accumulation of gold along two stages of formation. The first stage accompanied the granitic intrusion where the mafic ultramafic rocks were heated and gold was mobilized to the heat source. The second stage is the intrusion of these quartz veinlets. The ore bodies of the vein type represent fissure fillings with some wall rock alterations in their vicinity.

2.1. *Geochemistry*

The chemical analysis for the granite samples under investigation has been done in order to identify their geochemical behavior. The chemical analysis for the major oxides (wt %) were done, using wet chemical analysis technique. The trace elements (ppm) were measured by XRF technique. All these chemical analyses were done in the Nuclear Materials Authority of Egypt. Table 1 shows the chemical analysis for major oxides and trace elements as well as some geochemical ratios for the studied monzogranites and syenogranites. The studied granites are, generally, characterized by their relatively high silica and Ba contents. Generally, the monzogranites are characterized by their relatively higher contents of FeO, Fe_2O_3, MgO, MnO, CaO, Sr and Ba as well as lower SiO_2, K2O, Rb, Zr, Y, Nb and F- contents than those of the syenogranite.

The potassic feldspars are responsible for the increase in Ba and Rb, while zircon is responsible for high concentration of Hf content. The gold mineralization hosted in these granodiorites is responsible for the higher contents of ore elements, Cr, Co, Ni, Cu, Zn, As, Sn, Sb, confirming that these are evidence for elements form the geochemical association of the gold mineralization.

3. Experimental procedure and methods

3.1. *Sampling preparation*

Twenty samples (12 quartz-bearing gold and 8 granite samples) were collected from investigated area. The samples were crushed, homogenized and sieved through a 200-mm mesh, which is the optimum size enriched in heavy minerals. Each sample was dried in an oven a 110 °C to ensure that moisture was completely removed. Weighed samples were placed in a polyethylene beaker, of 350 cm^3 volume each. The beakers were completely sealed for 4 weeks to reach secular equilibrium where the rate of decay of the progeny becomes equal to that of the parent (radium and thorium) within the volume and the progeny will also remain in the sample (ASTM, 1983; 1986).

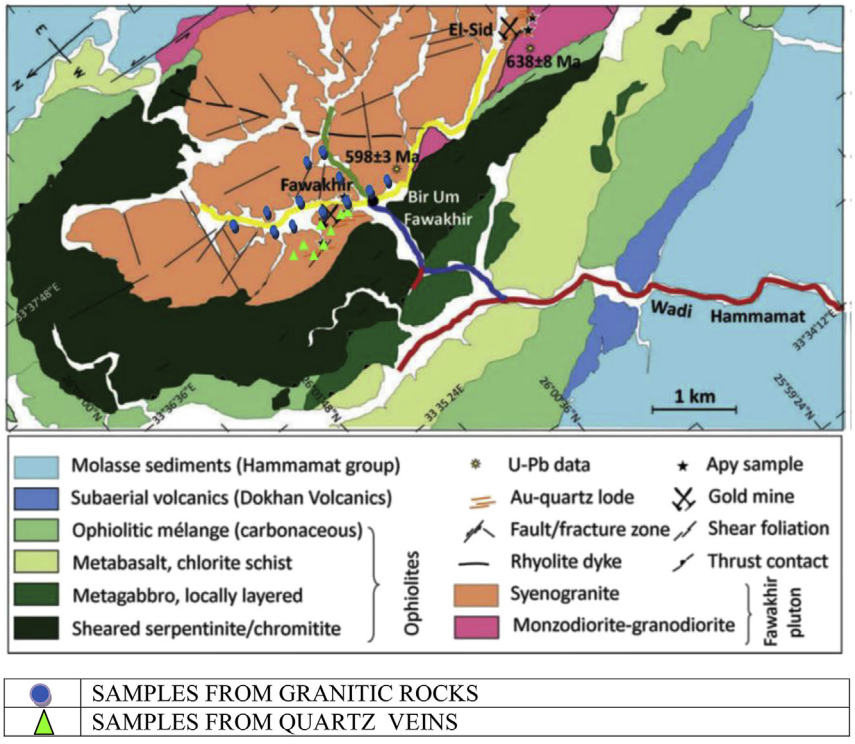

Fig. 1 – Geological and location map of El-Fawakhir area.

Table 1 – Major elements (oxides wt.%) and trace elements (ppm) of the studied granotoid.

S. No	G1	G2	G3	G4	G5	G6	G7	G8
SiO_2	73.80	65.00	66.00	74.80	65.35	63.34	74.00	74.00
TiO_2	0.20	0.92	0.86	0.14	0.60	0.70	0.05	0.03
Al_2O_3	14.00	16.76	16.61	13.33	16.49	16.23	14.30	13.75
Fe_2O_3	1.40	2.55	2.00	1.13	1.85	3.51	1.11	1.31
FeO	0.45	2.31	2.54	0.23	3.00	1.33	0.33	0.53
MnO	0.07	0.15	0.22	0.02	0.17	0.08	0.11	0.02
MgO	0.05	1.46	1.41	0.22	1.56	3.81	0.10	0.07
CaO	0.40	3.33	2.53	0.51	3.98	4.40	0.40	0.51
Na_2O	4.00	4.00	3.77	4.10	3.00	4.22	3.95	4.43
K_2O	4.77	4.54	4.00	3.97	4.61	4.43	4.12	4.36
P_2O_5	0.01	0.26	0.25	0.11	0.21	0.22	0.10	0.01
L.O.I	0.70	0.45	0.74	0.70	0.93	0.50	0.60	0.80
Total %	99.85	99.73	99.93	99.26	99.75	99.77	99.17	99.82
Trace elements (ppm)								
Au	2.01	1.6	1.57	1.9	1.41	2.20	1.67	1.73
Cr	21	21	22	14	15	15	18	16
Ni	11	8	7	5	6	7	5	7
Cu	10	10	11	11	11	10	13	10
Zn	57	55	57	70	43	35	54	58
Zr	165	100	158	193	124	94	147	115
Rb	70	70	69	53	83	60	56	71
Y	23	15	14	16	16	10	10	13
Ba	456	555	435	519	480	765	400	546
Pb	11	14	14	6	13	12	14	11
Sr	525	663	330	428	306	461	571	397
Ga	17	15	14	17	14	12	17	18
V	15	10	11	27	7	6	11	9
U ppm	6.4	4.9	5.5	4.9	4.8	5.2	5.5	6.6
Th ppm	88	24.3	32.7	38	34.12	27	45	42

3.2. Instrumentation and calibration

Activity measurements were performed by gamma ray spectrometer, employing a scintillation detector (3″ × 3″). It is hermetically sealed assembly, which includes a NaI (Tl) crystal, coupled to PC-MCA, CANBERRA Company (USA). To reduce gamma ray background, a cylindrical lead shield (100 mm thick) with a fixed bottom and movable cover shielded the detector. The lead shield contained an inner concentric cylinder of copper (0.3 mm thick) in order to absorb X-rays generated in the lead. In order to determine the background distribution in the environment around the detector, an empty sealed beaker was counted in the same manner and in the same geometry as the samples. The measurement time of activity or background was 43,200s. The background spectra were used to correct the net peak area of gamma rays of measured isotopes. The online analysis of each measured gamma-ray spectrum has been carried out by a dedicated software program (Genie, 2000) from Canberra Company (USA).

3.2.1. Calculation of activity

Calculations of count rates for each detected photo peak and radiological concentrations (activity per mass unit or specific activity) of detected radionuclides depend on the establishment of secular equilibrium in the samples. The ^{232}Th concentration was determined from the average concentrations of ^{212}Pb (238.6 keV) and ^{228}Ac (911.1 keV) in the samples, and that of ^{226}Ra was determined from the average concentrations of the ^{214}Pb (351.9 keV) and ^{214}Bi (609.3 and 1764.5 keV) decay products. The activity concentration in Bqkg^{-1} (A) in the environmental samples was obtained as follows (Shams, Mohamed, & Elsaman, 2012):

$$A = \frac{N_p}{e \times \eta \times m} \quad (1)$$

where Np = the (cps) sample − (cps) B.G, e is the abundance of the γ-line in a radionuclide, η is the measured efficiency for each gamma-line observed for the same number of channels either for the sample or the calibration source, and m the mass of the sample in kilograms. The minimum detectable activity concentrations were 25.2 Bqkg^{-1} for ^{40}K, 6.5 Bqkg^{-1} for ^{226}Ra and 5.7 Bqkg^{-1} for ^{232}Th. All procedures were described in previous publication (Uosif, 2007).

3.2.2. Radium equivalent activity

Radium equivalent concentration (Ra_{eq}) is a common index used to compare the specific activities of materials containing ^{226}Ra, ^{232}Th, and ^{40}K. It can be expressed It can be expressed (UNSCEAR 1982) as:

$$Ra_{eq} = A_{Ra} + 1.43A_{Th} + 0.077A_K \quad (2)$$

where, A_{Ra}, A_{Th} and A_K are specific activities (Bqkg^{-1}) of ^{226}Ra, ^{232}Th and ^{40}K respectively, Radium equivalent concentration (Ra_{eq}) was calculated based on the estimation that 370 Bqkg^{-1} of ^{226}Ra, 259 Bqkg^{-1} of ^{232}Th and 4810 Bqkg^{-1} of ^{40}K produce the same γ-ray dose rate (Yu, Guan, Stoks, & Young, 1992).

3.2.3. Absorbed dose rates (D_0)

The absorbed dose rates due to gamma radiations in air at 1 m above the ground surface for the uniform distribution of the naturally occurring radionuclides (^{226}Ra, ^{232}Th and ^{40}K) were calculated based on guidelines provided by (ICRP-60):

$$D_\circ = 0.427C_{Ra} + 0.662C_{Th} + 0.043C_K \quad (3)$$

where C_{Ra}, C_{Th} and C_K are the concentration in (BqKg^{-1}) of radium, thorium and potassium respectively (Shams et al., 2013).

3.2.4. External hazard index (H_{ex})

The external hazard index (H_{ex}) due to the emitted gamma rays for each sample was calculated according to the following formula (UNSCEAR, 1988):

$$H_{ex} = \frac{C_{Ra}}{370} + \frac{C_{Th}}{259} + \frac{C_K}{4810} \leq 1 \quad (4)$$

where C_{Ra}, C_{Th}, and C_K are the activity concentration of ^{226}Ra, ^{232}Th, and ^{40}K, respectively.

3.2.5. Annual effective dose rate (AEDR)

The gamma absorbed doses in nGy h^{-1}were converted to annual effective dose in mSvy^{-1} as proposed by (UNSCEAR, 2000). The annual effective dose rate (AEDR) was calculated by using the following equation.

$$AEDR = ADRA \times DCF \times OF \times T \quad (5)$$

where ADRA, DCF, OF are absorbed dose rate in air (nGy h^{-1}), dose conversion factor.

(0.7 Sv Gy^{-1}), outdoor occupancy factor (0.2) and the time, respectively (8760 hy^{-1}).

3.2.6. Excess lifetime cancer risk (ELCR)

Excess lifetime cancer risk (ELCR) was calculated also and listed in coulomb (5) in Table 3 by using the fowling equation (Taskin et al., 2009):

Table 2 – Activity concentrations of ^{226}Ra, ^{232}Th and ^{40}K in different samples.

Sample name	Activity in Bqkg^{-1}		
	^{226}Ra	^{232}Th	^{40}K
Q1	21 ± 1	34 ± 2	304 ± 15
Q2	14 ± 1	30 ± 1	155 ± 8
Q3	10 ± 1	38 ± 2	159 ± 8
Q4	32 ± 2	41 ± 2	140 ± 7
Q5	14 ± 2	17 ± 3	229 ± 14
Q6	37 ± 3	22 ± 3	282 ± 16
Q7	29 ± 1	12 ± 1	663 ± 33
Q8	25 ± 1	35 ± 2	595 ± 30
Q9	23 ± 2	20 ± 4	415 ± 22
Q10	33 ± 2	14 ± 2	201 ± 12
Q11	29 ± 2	25 ± 3	682 ± 35
Q12	12 ± 1	15 ± 1	221 ± 12
G1	15 ± 1	15 ± 1	128 ± 6
G2	15 ± 1	16 ± 1	319 ± 16
G3	36 ± 3	28±	391 ± 20
G4	43 ± 2	27 ± 1	388 ± 19
G5	35 ± 3	29 ± 3	374 ± 19
G6	15 ± 2	9 ± 1	174 ± 10
G7	35 ± 3	13 ± 2	212 ± 12
G8	37 ± 3	22 ± 3	282 ± 16

Table 3 – Radium equivalent (Ra_{eq}), the dose rate (D_o), external hazard indices (Hex), annual effective dose rate (AEDR), and excess lifetime cancer risk (ELCR).

Sample name	Ra_{eq} ($Bqkg^{-1}$)	D_o ($nGyh^{-1}$)	H_{ex} ($nGyh^{-1}$)	AEDR μSvy^{-1}	ELCR
Q1	91.0	44.6	0.3	54.1	1.89×10^{-4}
Q2	67.1	32.2	0.2	39.1	1.37×10^{-4}
Q3	75.5	36.3	0.2	44.1	1.54×10^{-4}
Q4	45.5	21.9	0.1	26.6	9.30×10^{-5}
Q5	54.2	27.0	0.2	32.8	1.15×10^{-4}
Q6	59.5	30.4	0.2	36.9	1.29×10^{-4}
Q7	92.6	48.9	0.3	59.3	2.08×10^{-4}
Q8	116.7	59.4	0.3	72.9	2.63×10^{-4}
Q9	81.3	41.2	0.2	50.0	1.75×10^{-4}
Q10	40.3	20.0	0.1	24.2	8.48×10^{-5}
Q11	112.8	58.4	0.3	70.9	2.48×10^{-4}
Q12	48.9	24.6	0.1	30.1	8.85×10^{-5}
G1	100.3	46.8	0.3	56.8	1.99×10^{-4}
G2	87.6	42.2	0.2	51.3	1.80×10^{-4}
G3	104.3	51.1	0.3	62.1	2.17×10^{-4}
G4	108.4	52.7	0.3	64.1	2.24×10^{-4}
G5	102.5	50.2	0.3	60.9	2.13×10^{-4}
G6	67.4	32.2	0.2	39.1	1.37×10^{-4}
G7	69.0	32.9	0.2	39.9	1.40×10^{-4}
G8	87.6	42.2	0.2	51.3	1.80×10^{-4}

$$ELCR = AEDE \times DL \times RF \quad (6)$$

where AEDE is the annual effective dose equivalent, DL is duration of life (70 year) and RF is risk factor (Sv^{-1}) fatal cancer risk per Sievert. For stochastic effects, ICRP 60 uses values of 0.05 for the public.

4. Results and discussion

This study is a continuation of our ongoing project in physics department (Faculty of Science, Al-Azher University, Assuit Branch, Egypt) related to the measurement of specific activity of ^{226}Ra, ^{232}Th and ^{40}K in environmental samples from Upper Egypt using a gamma-ray spectrometric technique and estimation of the gamma dose rate from these radionuclides. The obtained results of the measured specific activities in different samples which listed in Table 2 show that the values the highest ^{226}Ra, ^{232}Th and ^{40}K concentrations are 43 ± 2, 41 ± 2 and 682 ± 35 ($BqKg^{-1}$) respectively and the minimum concentrations are 10 ± 1, 9 ± 1 and 128 ± 7 ($BqKg^{-1}$) respectively. The variations of natural radioactivity levels at different samples are due to the variation of concentrations of these elements in the geological formations. The obtained results for ^{226}Ra are lower than the average international radioactivity levels, which is 35 $Bqkg^{-1}$ (UNSCEAR, 1993) except in sample G5 reaching 43 $Bqkg^{-1}$. The ^{232}Th results are lower in all locations than the average international radioactivity levels of 50 $Bqkg^{-1}$. The content of Th generally increases with SiO_2 content and closely follows U during differentiation or partial melting. The increase in U with both SiO_2 and alkali content is usually more marked than the increase in Th. The ^{40}K results are also lower in all locations than the average international radioactivity levels of 500 $Bqkg^{-1}$ except in three quartz samples, which named Q7,Q8 and Q11 reaching 663, 595, and 682 respectively $Bqkg^{-1}$.

Generally the presence of such high radioactivity in the granites may be attributed to the presence of relatively increased amount of accessory minerals such as zircon, iron oxides, fluorite and other radioactive related minerals. The radioactive related minerals play an important role in controlling the distribution of uranium and thorium. Zircon usually contains uranium and thorium concentration ranging from 0.01% to 0.19%, 1%–2%, respectively.

The obtained results of Ra_{eq} in Table 3 showed that, the lowest value Ra_{eq} was 40.3 $Bqkg^{-1}$ where the highest one was 112.8 $Bqkg^{-1}$. The maximum value (UNSCEAR 1993) of Ra_{eq} in granite samples must be less than 370 $Bqkg^{-1}$ to keep the external dose below 1.5 $mSvy^{-1}$.These values are less than the maximum admissible (UNSCEAR, 2000) value of 370 $Bqkg^{-1}$.

The absorbed dose rate values which extracted from the concentration values of ^{226}Ra, ^{232}Th and ^{40}K in ($BqKg^{-1}$) were listed in Table 3. It shows that the lowest dose rate is 20 $nGyh^{-1}$, while the highest dose rate was 58.4 $nGyh^{-1}$ for granite samples. Studies indicate an average outdoor terrestrial gamma dose rate is 60 $nGyh^{-1}$, it is lower than the global average values ranging from 10 to 200 $nGyh^{-1}$ (UNSCEAR, 2000). In the other hand the calculated external hazard index (H_{ex}) was found to be less than unity as shown in Table 3.

The calculated annual effective dose rate (AEDR) values were varied from 24.2 to 72.9 μSvy^{-1}, these values are in the same global average outdoor terrestrial radiation value of 0.07 mSv y^{-1} reported by UNSCEAR, 2000. The highest excess lifetime cancer risk value for the granite samples as shown in Table 3 was 2.5×10^{-4}, while the lowest ELCR value was 8.48×10^{-5} with average value (1.61×10^{-4}), this value is lower than average world value (2.9×10^{-4}) (ICR-90, 1990). Yet we were not able to evaluate the health hazards of the assessed values on the population. Since reliable, standardized

mortality and morbidity statistics were not accessible, this study was limited to background radiation levels.

5. Conclusion

The values of measured specific activities of natural radionuclides ^{226}Ra, ^{232}Th and ^{40}K in investigated samples are within the acceptable limits. The average values of all the calculated radiological indices extracted from these activities, in all investigated samples are within the levels recommended by UNSCEAR, 2000 report. The data obtained here are reference values to be used as a data baseline for drawing a radiological map of El-Fawakhir area.

Acknowledgment

This work was carried out using the nuclear analytical facilities at the Physics department, Faculty of Sciences, Al-Azhar University, Assiut, Egypt.

REFERENCES

American Society for Testing Materials (ASTM). (1983). *Standard method for sampling surface soils for radionuclides*. Report No. C. ASTM (pp. 983–998).

American Society for Testing Materials (ASTM). (1986). *Recommended practice for investigation and sampling soil and rock for engineering purposes*. Report No. D Ann. Book of ASTM Standards (04.08) 420, ASTM (pp. 109–113).

Amer, R. M., Kusky, T. M., & Ghulam, A. (2008). New methods of processing ASTER data for lithological mapping: examples from Fawakhir, Central Eastern Desert of Egypt. *Journal of African Earth Sciences*.

El-Shazly, E. M. (1956). *Notes on the mining map of Egypt*. Repts of 20th International Geol. Congress, Mexico Assoc. African Geol. Surveys (pp. 423–437).

Faure, G. (1986). *Principles of isotope geology* (2nd ed.). New York: Wiley, ISBN 0471864129.

GENIE-2000. (1997). *Basic spectroscopy (Standalone) V1.2A, Copyright (c), Canberra Industries*.

Hassan, M. M. (2006). Gold deposits in Egypt a renewing resource for National income. In *The Ninth Arab conference for mineral resources, Kingdom of Saudi Arabia-Jeddah, 30, Oct.-1 Nov. 2006*.

Hassan, M. M., Azzaz, S. A., Soliman, M. M., & El-Badway, E. (1991). *Use of some statistical and geochemical parameters in solving some genetic problem of Sukkari gold mineralization*. Egypt 48th I-S.1. Session, Cairo, 9–17 Sep., 1991.

ICRP-60. (1991). International Commission on Radiological Protection Recommendations of the International Commission on Radiological Protection. *Annals of the ICRP, 21*, 1–3.

Mason, B., & Moore, C. B. (1982). *Principles of geochemistry* (4th ed.). New York: Wiley.

Me'nager, M., Heath, M., Ivanovich, M., Montjotin, C., Barillon, C., Camp, J., et al. (1993). Migration of uranium from uranium-mineralised fractures into the rock matrix in granite: implications for radionuclide transport around a radioactive waste repository. In *4th International Conference of Chemistry and Migration Behaviour of Actinides and Fission Products in the Geosphere (Migration, 1993), Charleston, USA* (pp. 47–83), 12–17, December 1993, Radiochim. Acta 66/67.

Rudnick, R.l., & Gao, S. (2003). Composition of the continental crust. In *Treatise on geochemistry* (Vol. 3, pp. 1–64). Amsterdam: Elsevier.

Sabet, A. H., Tosgeov, V. B., Bordonosov, V. P., Baburin, L. M., & Zalta, A. (1976). On gold mineralization in the eastern desert of Egypt. *Annals of the Geological Survey of Egypt, VI*, 201–212.

Shams, I. S. S. A., Mohamed, U. O. S. I. F., & Elsaman, R. (2013). Gamma radioactivity measurements in Nile River sediment samples. *Turkish Journal of Engineering and Environmental Sciences, 37*, 109–122.

Taskin, H., Karavus, M., Ay, P., Topuzoglu, A., Hindiroglu, S., & Karahan, G. (2009). Radionuclide concentrations in soil and lifetime cancer risk due to the gamma radioactivity in Kirklareli, Turkey. *Journal of Environmental Radioactivity, 100*, 49–53.

UNSCEAR. (1982). *Ionizing radiation: Sources and biological effects*. New York: United Nations Scientific Committee on the Effects of Atomic Radiation.

UNSCEAR. (1988). *Sources, effects and risks of ionizing radiation*. Report to the General Assembly on the Effects of Atomic Radiation, United Nations, New York. United Nations Scientific Committee on the effects of atomic radiation.

UNSCEAR. (1993). *Sources and effects of ionizing radiation*. New York: United Nations Scientific Committee on the Effects of Atomic Radiation.

UNSCEAR. (2000). *Sources and effects of ionizing radiation*. Report of the United Nations Scientific Committee on the Effects of Atomic Radiation to the GeneralAssembly, United Nations, New York.

Uosif, M. A. M. (2007). Gamma-ray spectroscopic analysis of selected samples from Nile river sediments in Upper Egypt. *Radiation Protection Dosimetry, 123*, 215–220.

Uosif, M. A. M., & Abdel-Salam, L. M. (2011). An assessment of the external radiological impact in granites and pegmatite in central eastern desert in egypt with elevated natural radioactivity. *Radiion Protection Dosimetry, 147*(3), 467–473.

Yu, K. N., Guan, Z. J., Stoks, M. J., & Young, E. C. (1992). The assessment radiation of natural radiation dose commited to the Hong Kong people. *Journal of Environmental Radioactivity, 17*, 931.